(6) E. R. Garrett and P. B. Chemburkar, *J. Pharm. Sci.*, **57**, 944(1968).

(7) *Ibid.*, **57**, 949(1968).

(8) *Ibid.*, **57**, 1401(1968).

(9) M. Nakano and N. K. Patel, *J. Pharm. Sci.*, **59**, 79(1970).

(10) J. Haleblian, R. Runkel, N. Mueller, J. Christopherson, and K. Ng, *ibid.*, **60**, 541(1971).

(11) C. F. Most, *J. Appl. Polym. Sci.*, **14**, 1019(1970).

(12) G. L. Flynn and T. J. Roseman, *J. Pharm. Sci.*, **60**, 1788 (1971).

(13) G. L. Flynn and R. W. Smith, *ibid.*, **61**, 61(1972).

(14) T. J. Roseman and W. I. Higuchi, *ibid.*, **59**, 353(1970).

(15) T. J. Roseman, *ibid.*, **61**, 46(1972).

(16) T. Higuchi, *ibid.*, **52**, 1145(1963).

(17) B. J. Zwolinski, H. Eyring, and C. E. Reese, *J. Phys. Chem.*, **53**, 1426(1949).

(18) R. E. Beck and J. S. Schultz, *Science*, **170**, 1302(1970).

(19) J. Dainty and C. R. House, *J. Physiol.*, **182**, 66(1966).

(20) A. W. Cuthbert and Y. Dunant, *Brit. J. Pharmacol.*, **40**, 508(1970).

(21) G. L. Flynn and E. W. Smith, *J. Pharm. Sci.*, **60**, 1713 (1971).

(22) H. C. Brill, *J. Amer. Chem. Soc.*, **43**, 1320(1921).

(23) G. L. Flynn, *J. Pharm. Sci.*, **60**, 345(1971).

(24) T. Higuchi and S. S. Davis, *ibid.*, **59**, 1376(1970).

(25) G. Saracco and E. S. Marchetti, *Ann. Chim.*, **48**, 1357(1958).

(26) H. A. Daynes, *Proc. Roy. Soc.*, *Ser. A*, **97**, 286(1920).

(27) R. M. Barrer, *Trans. Faraday Soc.*, **35**, 628(1939).

(28) K. F. Finger, A. P. Lemberger, T. Higuchi, L. W. Busse, and D. E. Wurster, *J. Amer. Pharm. Ass., Sci. Ed.*, **49**, 569(1960).

(29) W. I. Higuchi and T. Higuchi, *ibid.*, **49**, 598(1960).

(30) G. L. Flynn, O. S. Carpenter, and S. H. Yalkowsky, *J. Pharm. Sci.*, **61**, 312(1972).

(31) S. H. Yalkowsky, G. L. Flynn, and T. G. Slunick, *ibid.*, **61**, 852(1972).

(32) I. D. Robb, *Austr. J. Chem.*, **19**, 2281(1966).

(33) J. J. Kipling, "Adsorption from Solutions of Nonelectrolytes," Academic, New York, N. Y., 1965, pp. 179–187.

(34) E. G. Klarmann, V. A. Shternov, and W. L. Gates, *J. Lab. Clin. Med.*, **20**, 40(1934).

(35) J. B. Niederl, V. Niederl, S. Shapiro, and M. E. McGreal, *J. Amer. Chem. Soc.*, **59**, 1113(1937).

(36) R. R. Read and E. Miller, *ibid.*, **54**, 1195(1932).

(37) W. I. Higuchi, *J. Pharm. Sci.*, **56**, 315(1967).

(38) R. Adams, E. K. Rideal, W. B. Burnett, R. L. Jenkins, and E. E. Dreger, *J. Amer. Chem. Soc.*, **48**, 1758(1926).

(39) K. Kakemi, T. Arita, R. Hori, and R. Konishi, *Chem. Pharm. Bull.*, **15**, 1883(1967).

(40) K. Kakemi, T. Arita, R. Hori, R. Konishi, and K. Nishimura, *ibid.*, **17**, 248(1969).

(41) R. Zahradnik, *Arch. Int. Pharmacodyn. Ther.*, **135**, 311 (1962).

(42) K. Kakemi, T. Arita, S. Kitazawa, M. Kawamura, and H. Takenaka, *Chem. Pharm. Bull.*, **15**, 1819(1967).

(43) K. Kakemi, T. Arita, R. Hori, and R. Konishi, *ibid.*, **15**, 1534(1967).

(44) "The Merck Index," 7th ed., Merck & Co., Rahway, N. J., 1960, p. 119.

(45) M. Mayerson and M. Gibaldi, *J. Pharm. Sci.*, **58**, 1429(1969).

(46) *Ibid.*, **60**, 225(1971).

Importance of Chain Length on Physicochemical and Crystalline Properties of Organic Homologs

S. H. YALKOWSKY▲, G. L. FLYNN, and T. G. SLUNICK

Abstract ☐ It has been observed that certain physical properties of normal alkyl *p*-aminobenzoates (*i.e.*, their melting behavior and their solubilities in water, silicone oil, and hexane) exhibit an unusual dependency upon chain length. Each property is characterized by a definite break in the chain length profile about the butyl ester. However, the silicone oil–water and hexane–water partition coefficients of these esters show a regular increase with chain length extending over many orders of magnitude. The overall behavior of these homologs is attributed to basic difference in the crystal lattices of short (≤four carbons) and long (≥four carbons) homologs. X-ray patterns and thermal data were obtained and are supportive of this conclusion. As an additional verification, the hexane solubility of each compound was calculated by Scatchard–Hildebrand theory using the thermal data and empirically estimated solubility parameters. Agreement between calculated and experimental values is excellent. Because of relationships drawn for the influence of chain length on solubility and relative solubility (partition coefficients), these experiments also indicate a convenient method of estimating congeneric solubilities in other solvents.

Keyphrases ☐ Alkyl *p*-aminobenzoates—effect of chain length on melting point, solubilities, partition coefficients, crystalline properties ☐ Homologous alkyl series, *p*-aminobenzoates—effect of chain length on melting point, solubilities, partition coefficients, crystalline properties ☐ Chain length effect— melting point, solubilities, partition coefficients, and crystalline properties of alkyl *p*-aminobenzoates ☐ Structure–activity relationships —effect of alkyl chain length on physicochemical and crystalline properties, *p*-aminobenzoate esters

The importance of a drug's physical–chemical properties in determining its biological and pharmaceutical characteristics has long been recognized. Of particular importance are the aqueous solubility and the partition coefficient which are the major determinants of a drug's dissolution, distribution, and availability. An under-

Table I—Melting Points of Alkyl *p*-Aminobenzoates

Ester	Hot Stage	DSC	Literature (8)
Methyl	112°	112°	112–114°
Ethyl	89°	90°	90–91°
Propyl	74°	73°	74–91°
Butyl	56°	56°	58–59°
Pentyl	52°	53°	53–54°
Hexyl	61°	61°	62–64°
Heptyl	75°	49°, 76°ᵃ	75–77°
Octyl	71°	70°, 72°ᵇ	70–72°
Nonyl	69°	68°	—
Dodecyl	82°	82°	—
Hexadecyl	87°	79°, 85°ᵇ	—

ᵃ Endotherm at 49° is not present in cooling curve or in remelting curve. ᵇ Shoulder on major endotherm.

Figure 1—*Melting points of alkyl* p-*aminobenzoates.*

standing of the manner in which these and other properties change within a homologous series, *i.e.*, with incremental additions of methylene units, can be of use in choosing a derivative having optimum properties.

In this regard, the physical–chemical properties of a homologous series of alkyl *p*-aminobenzoates were investigated. This series was chosen because: (*a*) its biological activity was studied previously by a number of workers (1–5), giving baseline data for possible correlations, and (*b*) the needed compounds were previously synthesized for another study (1). Because they are biologically active, have an ionizable amine function and a strong UV chromophore, and cover a wide range of hydrophobicity, these compounds are well suited as a model series for structure–activity studies.

The relative solubilities of the members of the *n*-alkyl *p*-aminobenzoates are atypical of a homologous series. However, it will be shown that the solubility data can be correlated with the anomolous melting, crystallographic, and thermal properties of the respective congeners.

EXPERIMENTAL

Materials—*p*-Aminobenzoic acid[1], methyl *p*-aminobenzoate[1], and ethyl *p*-aminobenzoate[1] were used as received. All other esters used in this study were synthesized from the appropriate alcohol[2] and *p*-nitrobenzoyl chloride[3], as described previously (1). In the solubility studies, reagent grade hexane[1] and a silicone oil[4] (20 cSt. viscosity grade) were used.

Melting Points—The melting points of all of the esters prepared were determined by the following two independent methods: (*a*) controlled heating on a Mettler hot stage with digital readout, and (*b*) differential scanning calorimetry with the melting point determined as the temperature at which melting begins by extrapolating the initial segment of the endotherm to the baseline. The values determined by these two methods and the available literature values, for comparative purposes, are shown in Table I.

Aqueous Solubility—The aqueous solubilities of these esters were determined at 37°, as described in *Reference 1*, by either UV spectrophotometric or GC assay.

Silicone Oil and Hexane Solubility—The hexane and silicone oil solubilities were obtained by equilibrating an excess of *p*-aminobenzoic acid ester in the solvent for 3 days at 37°. The saturated solutions were then diluted with hexane, and the absorbance at 293 nm. was determined against a similarly prepared blank using a UV spectrophotometer[5]. The molar absorptivities at 293 nm. were determined in standard hexane solutions.
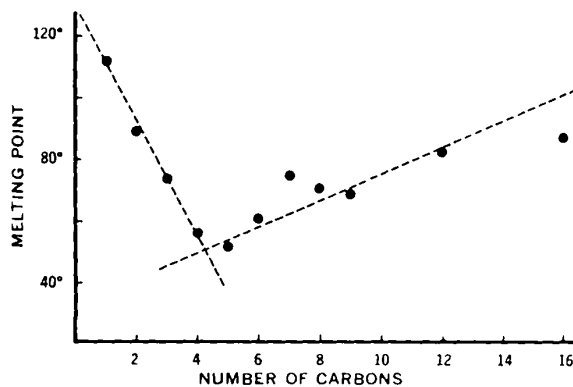
X-Ray Diffraction—The X-ray diffraction patterns of powdered samples of each ester were determined on an X-ray spectrophotometer[6]. The *d* spacings were calculated from the diffraction angle, *θ*, and the $K\alpha_1$ wavelength for a copper target (λ = 1.54050 Å).

Differential Scanning Calorimetry (DSC)—The heat of fusion, ΔH_f, and the entropy of fusion, ΔS_f, were determined on a DSC cell[7] connected to a differential thermal analyzer console[8] equipped with an *X-Y* recorder.

An accurately weighed sample (between 400 and 800 mg.) was placed on the sample thermocouple and maintained in a nitrogen atmosphere throughout the experiment. All samples were heated at 10°/min. The heating curves were recorded at 10°/in. (2.54 cm.) and an instrument sensitivity of 1.0. The molar heats of fusion were calculated by multiplying the area of the melting endotherm by 160, the previously determined heat transfer coefficient of the cell, and then dividing by the number of moles of sample used. The entropy of fusion of each compound was determined by dividing the heat of fusion by the absolute temperature of melting, T_m.

RESULTS

Melting Point—The melting points of the *p*-aminobenzoic acid esters determined by DSC are shown in Fig. 1. As chain length is increased, the melting point decreases almost linearly to the butyl ester and then increases gradually and irregularly. Thus, a change
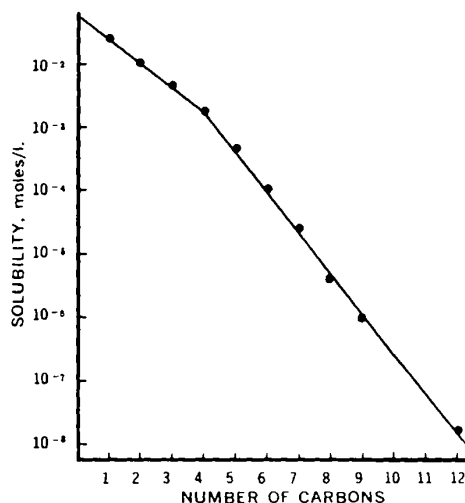

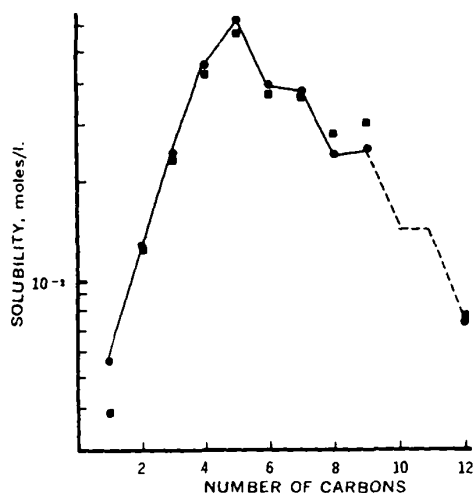**Figure 2**—*Solubility of alkyl* p-*aminobenzoates in water at 37°.*

Figure 3—*Solubility of alkyl p-aminobenzoates in hexane at 37°· Key: ●, experimental values; and ■, values calculated by Eq. 4.*

in melting behavior relative to increasing chain length at the butyl ester is clearly evident. These trends are emphasized by the arbitrarily drawn lines in Fig. 1.

Solubility Studies—The logarithms of the 37° aqueous solubilities of the esters studied are plotted *versus* chain length in Fig. 2. The data appear to fall on two straight lines; p-aminobenzoic acid and its methyl, ethyl, propyl, and butyl esters fall on a line having a slope of −0.349, which corresponds to a 2.24-fold decrease in solubility per methylene unit. The solubility values for butyl and the remaining p-aminobenzoic acid esters describe a line having a slope of −0.625. The latter represents a 4.22-fold solubility decrease per methylene unit.

The solubilities of these esters were also studied at 37° in two organic solvents: dimethylpolysiloxane (silicone) oil and hexane. The semilogarithmic solubility profiles of the esters in these two solvents are given in Figs. 3 and 4. Unlike the aqueous solubilities, the organic phase solubilities of these esters increase linearly with chain length for short-chain esters and reach a maximum at about the butyl derivative. Thereafter, the solubilities in each of these solvents decrease irregularly. The positive slopes of the lines drawn through the solubility data for the short-chain esters are 0.19 and 0.31 for silicone oil and hexane, respectively. There is a definite odd–even alteration in the solubilities of the higher esters, with the average decrease in solubility per methylene unit being a factor of about 1.3 in silicone oil and 0.6 in hexane. There is roughly only a 10-fold variation in solubility from one carbon to 12 carbons in the
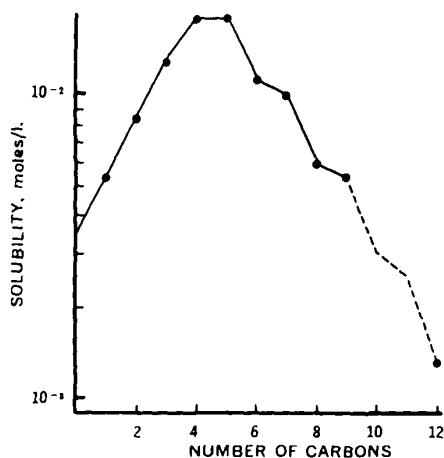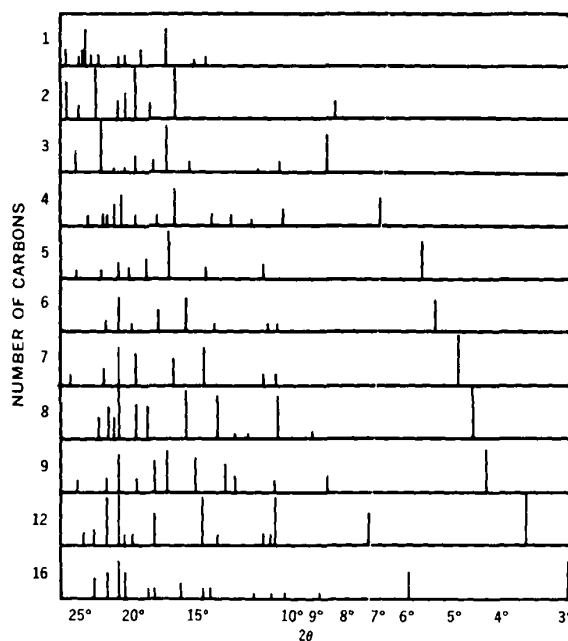

Figure 5—*X-ray diffraction patterns for alkyl p-aminobenzoates.*

organic phases. However, the variation in water is over a million-fold.

X-Ray Diffraction and Thermal Analysis—Each of the four sets of data presented shows a change in the chain length dependency at four carbons. Since it was presumed that the observed behavior was due to a fundamental change in the crystal properties, X-ray diffraction and thermal analyses were performed on the crystalline materials to get information on their dimensions and thermodynamic properties. The major spots of the X-ray diffraction patterns are summarized in Fig. 5. The angles reported for 2θ are plotted logarithmically to facilitate the detection of angle multiples. The intensities indicated are rough approximations of the true values.

The heat of fusion, ΔH_f, and the entropy of fusion, ΔS_f, of each ester are listed in Table II. Although there is considerable scatter in the data, plots of entropy and enthalpy of fusion indicate an essentially linear increase with chain length. The change in ΔS_f per methylene unit is 2.9 e.u. This increase is close to the value of 2.7 ± 0.1 e.u. characteristic of monoclinic crystals (6). (By contrast, the value for orthorhombic crystals is 2.3 ± 0.1 e.u. per methylene addition.)

DISCUSSION

Melting Point, Solubility, and Partition Coefficient—Silicone oil was used as a solvent in this study because of its chemical similarity to the more highly polymerized silicone rubber, which is a solid and

Figure 4—*Solubility of alkyl p-aminobenzoates in silicone oil at 37°.*

Table II—Thermal Properties of Alkyl *p*-Aminobenzoates

Ester	T_m, °K.	ΔH_f, kcal./mole	ΔS_f, e.u.
Methyl	385	5850	15.1
Ethyl	363	4720	13.1
Propyl	346	5070	14.6
Butyl	329	5870	17.8
Pentyl	326	5820	17.8
Hexyl	334	8450	25.2
Heptyl	349	6350	18.1
Octyl	345	9750	28.3
Nonyl	341	10800	31.4
Dodecyl	355	14700	41.5
Hexadecyl	358	19900	55.5

Table III—Solubilities and Partition Coefficients of Alkyl p-Aminobenzoates

Ester	Water Solubility, moles/l.	Silicone Oil Solubility, moles/l.	Oil–Water Partition Coefficient	Hexane Solubility, moles/l.	Oil–Water Partition Coefficient
Methyl	2.53×10^{-2}	5.25×10^{-3}	2.08×10^{-1}	5.67×10^{-3}	2.24×10^{-1}
Ethyl	1.02×10^{-2}	8.33×10^{-3}	8.17×10^{-1}	1.28×10^{-2}	1.25×10^{0}
Propyl	4.70×10^{-3}	1.29×10^{-2}	2.74×10^{0}	2.47×10^{-2}	5.25×10^{0}
Butyl	1.72×10^{-3}	1.78×10^{-2}	1.03×10^{1}	4.60×10^{-2}	2.68×10^{1}
Pentyl	4.50×10^{-4}	1.78×10^{-2}	3.95×10^{1}	6.30×10^{-2}	1.40×10^{2}
Hexyl	1.07×10^{-4}	1.12×10^{-2}	1.05×10^{2}	3.98×10^{-1}	3.72×10^{2}
Heptyl	2.50×10^{-5}	1.00×10^{-2}	4.00×10^{2}	3.81×10^{-1}	1.52×10^{3}
Octyl	4.00×10^{-6}	5.95×10^{-3}	1.48×10^{3}	2.46×10^{-1}	6.15×10^{3}
Nonyl	1.00×10^{-6}	5.34×10^{-3}	5.34×10^{3}	2.57×10^{-2}	2.57×10^{4}
Dodecyl	1.60×10^{-8}	1.31×10^{-3}	8.20×10^{4}	7.40×10^{-3}	4.64×10^{5}
Hexadecyl	—	—	—	7.20×10^{-3}	—

not well suited for partition coefficient studies. Dimethylpoly-siloxane membranes (silicone rubber) have been used by the authors (1, 7, 8) and others (9-12) for theoretical studies on membrane transport. A second organic solvent, hexane, was used to demonstrate the generality of the solubility profile and to provide assurance that the silicone oil data are not artifactual.

The solubilities of each ester studied in water, silicone oil, and hexane are given in Table III. These values provide estimates of the partition coefficients of each homolog between the immiscible phases. Although the solubilities of the esters cannot be described by a single exponential function of chain length in any of the three solvents, the logarithm of the partition coefficient (as estimated by the solubility ratio) is linearly dependent on chain length. Figure 6 shows this linearity and the absence of an inflection point at four carbons for both the silicone oil–water and the hexane–water partition coefficients. The data of Buchi *et al.* (5) for these esters indicate that the logarithms of the oleyl alcohol–water and amyl acetate–water partition coefficients also have a linear dependency on chain length through this range.

The change in log [partition coefficient] with chain length, *i.e.*, the slope of the lines of Fig. 6, is commonly designated as π. The π values for silicone oil and hexane are 0.54 and 0.66, respectively. If the negative slopes of the segment above four carbons (which are typical of most homologous series) of the logarithms of the aqueous and organic solvent solubilities are designated as $-\delta$ and $-\epsilon$, respectively, it can be seen that $\pi = (-\epsilon) - (-\delta) = \delta - \epsilon$. The value of δ is 0.625 for the alkyl p-aminobenzoates. Most homologous series have δ values very close to this value. The π values vary only slightly from series to series and even from nonpolar solvent to nonpolar solvent. Thus, it can be seen that the major contribution to the π value of a series is the change in aqueous solubility with chain length. Furthermore, the π value is usually around 0.5 for most nonpolar solvents.

The curves in Figs. 1–4 all show a sharp change in slope at the butyl derivative. Because melting points and solubilities of crystalline materials are heavily dependent upon crystal energies, it is proposed that the nonlinearity of these curves is due to a change in crystal structure with chain length. The crystal structure of the lower homologs is probably determined primarily by the aromatic ring and the dipolar nature of the p-aminobenzoic acid moiety. If chain length is increased beyond four carbons, the linear aliphatic chains begin to exert a dominating effect. The odd–even alteration seen in the melting point and organic solvent solubility, which is characteristic of long-chain compounds, supports this contention. The fact that no alteration is observed in the aqueous solubility data cannot be regarded as significant, since the error in solubility measurement is of sufficient magnitude to mask the expected odd–even alterations. The linearity (*i.e.*, lack of change in slope) of the data in Fig. 6 also supports this hypothesis, because the partition coefficient is a property of the solute and therefore is not dependent on crystal structure. Since the solubility in any solvent is dependent upon the sum of the energy required to disrupt the crystal and the intermolecular interactions between like and unlike species in solution, the solubility ratios are independent of the crystal disruption term which appears in the numerator and denominator (see section on DSC). Therefore, the partition coefficient is only dependent upon the interactions occurring in solution.

These facts provide the basis of the following convenient method for determining the aqueous solubility of very insoluble members of any homologous series, even if some or all of the congeners are crystalline. In a solvent for which the π value of a methylene unit is known, the solubility ratio of a short-chain derivative is determined. The solubility of the long-chain derivative is determined in the same solvent. This is usually possible because, as shown in the *Results* section, the solubility does not decrease greatly with chain length for most organic solvents. The logarithm of the solubility ratio plus πm, where m is the difference in the carbons between the short- and long-chain compounds, is equal to the logarithm of the solubility ratio of the insoluble congener. The aqueous solubility is then determined from the solubility ratio and the organic solvent solubility. This method can be used to predict the solubility profile of a series in one solvent from its solubility profile in another solvent and one solubility ratio.
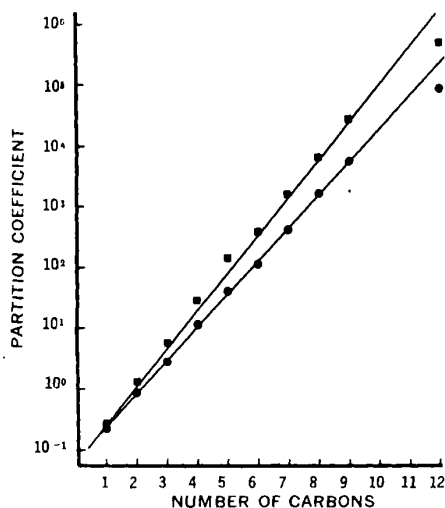

Figure 6—*Partition coefficients of alkyl* p-*aminobenzoates. Key:* ●, *silicone oil–water; and* ■, *hexane–water.*

Table IV—Group Contributions to Molar Volume and Molar Attraction Constants

Group	Volume, cm.^{3}/mole	$(E_2 V_2)^{1/2}$, cal.$^{1/2}$×cm.$^{3/2}$/mole
NH$_2$	7.7	423[a]
C$_6$H$_4$	64	658[b]
COO	15.9	310[b]
CH$_3$	32.4	214[b]
CH$_2$	16.2	133[b]
Ethyl p-aminobenzoate	144.2	1738[c]

[a] Determined by subtracting values of other components from 1738. [b] Small's values (22). [c] Determined from solubility in hexane.

Table V—Estimation of Solubility Parameters for Alkyl p-Aminobenzoates

Ester	V_2, cm.^{3}/mole	$(E_2V_2)^{1/2}$, cal.$^{1/2}$cm.$^{3/2}$/mole	δ_2, cal.$^{1/2}$/cm.$^{3/2}$
Methyl	128.0	1605	12.53
Ethyl	144.2	1738	12.05
Propyl	160.4	1871	11.69
Butyl	176.6	2004	11.53
Pentyl	192.8	2137	11.07
Hexyl	209.0	2270	10.86
Heptyl	225.2	2403	10.68
Octyl	241.4	2536	10.50
Nonyl	257.6	2669	10.39
Dodecyl	306.2	3068	10.01
Hexadecyl	371.4	3600	9.71

planar structure of methyl p-aminobenzoate

X-Ray Diffraction—To explore further the influences of the crystal structure, X-ray diffraction patterns were obtained for each ester. The patterns of Fig. 5 suggest a similarity in structure for the higher homologs. Based on the diffraction patterns, the lower derivatives are clearly distinctly different from the higher ones and from each other.

The easiest feature of each pattern to detect and interpret is the angle of least diffraction, *i.e.*, the spot or spike on the profile farthest to the right. This angle is related to the longest d spacing (the distance between adjacent molecular planes of the unit cell) of the crystal by:

$$d = \frac{a\lambda}{2\sin\theta} \quad \text{(Eq. 1)}$$

where a is a positive integer, λ is the wavelength of the X-irradiation, and θ is half the angle between the incident and diffracted rays. The d spacings increase linearly with chain length above four carbons, as can be seen from Fig. 7. The slope of the line (1.25 Å/methylene unit) is almost exactly what would be expected for a linear aliphatic chain (1.26 Å/methylene unit), assuming a tetrahedral angle of 109°, 28' and an interatomic distance of 1.54 Å (13). Furthermore, the values of these d spacings correspond almost exactly to the distance between the amine proton and the end methyl protons of a fully extended-scale molecular model of each higher homolog. The higher homologs all have a second d spacing of 4.1 Å which is common for aliphatic hydrocarbons. The longest d spacing of the lower homologs is less than the fully extended dimensions of the molecules. Methyl p-aminobenzoate has a length that would not allow the methyl group to be any farther from the amine group than the ester oxygen, suggesting Structure I. This structure would allow overlap of aromatic orbitals and also maxi-
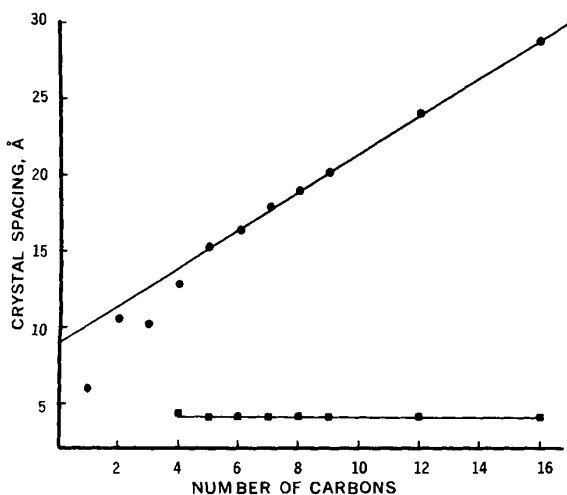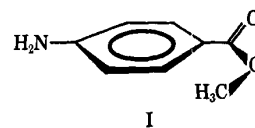

Figure 7—*Crystal spacings of alkyl* p-*aminobenzoates. Key: ●, long-est spacing; and ■, spacings along a second axis.*

mum dipole–dipole interactions between adjacent molecules. This would account for its high melting point and large energy and entropy of melting.

Thermal Analysis—If the change observed in the dependence of solubility upon chain length is related to crystal structure, it should be possible to correlate mathematically the solubility with the melting temperature, the heat of fusion, and the solubility parameter of each ester by the theory of regular solution (14–16). The mole fractional solubility, x_2, of a solid in an ideal solution is:

$$\log x_2 = \frac{-\Delta H_f}{4.575}\left(\frac{T_m - T}{T_m T}\right) + \Delta C_p\left[\frac{T_m - T}{4.575T} - \frac{\log}{1.987}\left(\frac{T_m}{T}\right)\right] \quad \text{(Eq. 2)}$$

where T_m and T are absolute melting point and temperature, respectively, and ΔC_p is the difference in heat capacity of the solid and the liquid form of the solute.

In a regular solution (14–16) (one in which heat is absorbed on mixing without any entropy change, other than the entropy of mixing, taking place), Eq. 2 must be modified to account for the intermolecular interactions which occur, giving:

$$\log x_2 = -\frac{\Delta H_f}{4.575}\left(\frac{T_m - T}{T_m T}\right) - \frac{V_2}{4.575T}(\delta_1 - \delta_2)^2\phi_1^2 + \Delta C_p\left[\frac{T_m - T}{4.575T} - \frac{\log}{1.987}\left(\frac{T_m}{T}\right)\right] \quad \text{(Eq. 3)}$$

where V_2 is the solute molar volume; δ_1 and δ_2 are the solubility parameters of the solvent and solute, respectively; and ϕ_1 is the volume fraction of solvent. Normally, ΔC_p is small (14) and the last term of Eq. 3 is ignored. Also, for materials of reasonably low solubility, ϕ_1 may be taken as unity. Thus, Eq. 3 becomes:

$$\log x_2 = -\frac{\Delta H_f}{4.575}\left(\frac{T_m - T}{T_m T}\right) - \frac{V_2}{4.575T}(\delta_1 - \delta_2)^2 \quad \text{(Eq. 4)}$$

Since the heat of fusion for each homolog has already been determined (Table II) and the solubility parameters of hexane and water are known to be 7.3 and 23.4, respectively (17), only V_2 and δ_2 must be known to calculate x_2.

The molecular volume of each ester can be calculated from its structure by the summation of group and atomic volumes (18–21). The molar volumes of the component groups of the alkyl p-aminobenzoates, taken from Yalkowsky (19) and Yalkowsky and Zografi (21), are given in Table IV. From these values it can be seen that the molar volume of the ethyl ester of p-aminobenzoic acid is 144.2 cm.^{3} and changes by 16.2 cm.^{3} per methylene group.

The solubility parameter of the solute, δ_2, which is defined as:

$$\delta_2 = \left(\frac{E_2}{V_2}\right)^{1/2} \quad \text{(Eq. 5)}$$

can be calculated by dividing the molar attraction constant $(E_2V_2)^{1/2}$ by V_2. The additivity of $(E_2V_2)^{1/2}$ is well established for hydrocarbons (22), but, unfortunately, there is no conclusive evidence for the additivity of $(E_2V_2)^{1/2}$ for polar groups (22). However, if a value of the molar attraction constant for one of the alkyl p-aminobenzoates can be determined, the values of $(E_2V_2)^{1/2}$ for the other esters can be estimated by adding 133 cal.$^{1/2}$ cm.$^{3/2}$ per methylene unit. The δ_2 value of ethyl p-aminobenzoate was determined from its hexane solubility, molar volume, melting point, and molar heat of fusion and Eq. 4 to be 12.05. The value of $(E_2V_2)^{1/2}$ for ethyl p-aminobenzoate was obtained by dividing δ_2 by V_2. The values of V_2, $(E_2V_2)^{1/2}$, and δ_2 derived from the values for the ethyl ester are shown in Table V. These values, along with the parameters already discussed, can now be incorporated into Eq. 4 to predict the hexane solubility of each ester. As can be seen from Table VI and Fig. 3,

DOCKET ALARM

Explore Litigation Insights

Docket Alarm provides insights to develop a more informed litigation strategy and the peace of mind of knowing you're on top of things.

Real-Time Litigation Alerts

Keep your litigation team up-to-date with **real-time alerts** and advanced team management tools built for the enterprise, all while greatly reducing PACER spend.

Our comprehensive service means we can handle Federal, State, and Administrative courts across the country.

Advanced Docket Research

With over 230 million records, Docket Alarm's cloud-native docket research platform finds what other services can't. Coverage includes Federal, State, plus PTAB, TTAB, ITC and NLRB decisions, all in one place.

Identify arguments that have been successful in the past with full text, pinpoint searching. Link to case law cited within any court document via Fastcase.

Analytics At Your Fingertips

Learn what happened the last time a particular judge, opposing counsel or company faced cases similar to yours.

Advanced out-of-the-box PTAB and TTAB analytics are always at your fingertips.

API

Docket Alarm offers a powerful API (application programming interface) to developers that want to integrate case filings into their apps.

LAW FIRMS

Build custom dashboards for your attorneys and clients with live data direct from the court.

Automate many repetitive legal tasks like conflict checks, document management, and marketing.

FINANCIAL INSTITUTIONS

Litigation and bankruptcy checks for companies and debtors.

E-DISCOVERY AND LEGAL VENDORS

Sync your system to PACER to automate legal marketing.

fastcase®
Smarter legal research.